J|A|C|S
ARTICLES
Published on Web 10/02/2004

QM/MM Studies of the Enzyme-Catalyzed Dechlorination of 4-Chlorobenzoyl-CoA Provide Insight into Reaction Energetics

Dingguo Xu,[†] Yanseng Wei,[†] Jingbo Wu,[†] Debra Dunaway-Mariano,[†] Hua Guo,*[,†] Qiang Cui,[‡] and Jiali Gao[§]

Contribution from the Department of Chemistry, University of New Mexico, Albuquerque, New Mexico 87131, Department of Chemistry, University of Wisconsin, Madison, Wisconsin 53706, and Department of Chemistry and Supercomputing Institute, University of Minnesota, Minneapolis, Minnesota 55455

Received July 5, 2004; E-mail: hguo@unm.edu

Abstract: The conversion of 4-chlorobenzoyl-CoA to 4-hydroxybenzoyl-CoA catalyzed by 4-chlorobenzoyl-CoA dehalogenase is investigated using combined QM/MM approaches. The calculated potential of mean force at the PM3/CHARMM level supports the proposed nucleophilic aromatic substitution mechanism. In particular, a Meisenheimer intermediate was found, stabilized by hydrogen bonds between the benzoyl carbonyl of the ligand and two backbone amide NHs at positions 64 and 114. Mutation of Gly113 to Ala significantly increases the barrier by disrupting the hydrogen bond with the Gly114 backbone. The formation of the Meisenheimer complex is accompanied by significant charge redistribution and structural changes in the substrate benzoyl moiety, consistent with experimental observations. Theoretical results suggest that the reaction rate is limited by the formation of the Meisenheimer complex, rather than by its decomposition. A kinetic model based on the calculated free energy profile is found to be consistent with the experimental time course data.

I. Introduction

Many strains of soil-dwelling bacteria degrade naturally occurring and synthetic halogenated organic compounds for energy production. Frequently, the halogen is removed from the organic unit by hydrolytic nucleophilic substitution prior to mineralization through classical oxidative pathways. Such is the case with 4-chlorobenzoate (4-CBA) catabolism, which begins with a three-step dehalogenation pathway leading to 4-hydroxybenzoate (4-HBA) and ends with the citric acid cycle, following oxidation through the ortho cleavage and β-ketoadipate pathways. The 4-CBA pathway is found in conjunction with polychlorinated biphenyl (PCB) oxidation pathways in naturally occurring and engineered bacterial PCB degraders, which produce 4-CBA as a toxic byproduct.

The key enzyme of the dehalogenation pathway, and the topic of this paper, is 4-chlorobenzoyl-coenzyme A (4-CBA-CoA) dehalogenase. This enzyme has attracted a great deal of attention, in part because of its remarkable mechanism of catalysis,[1−3] and in part because of its potential application in expanded bioremediation of toxic halogenated aromatic pollutants.[4,5] The current knowledge of this system, though incomplete, suggests that the enzyme takes advantage of several effective catalytic strategies, such as preorganization of the reactants in the active site,[6−8] solvation substitution,[9] and electrostatic and H-bonding stabilization of the transition state.[10,11] Therefore, the catalyzed reaction serves as an ideal prototype to dissect the contributions of these factors, which have been proposed to play roles with varying levels of importance in many other enzymatic reactions.[8,12−16] The elucidation of the catalytic mechanism and factors influencing the catalytic efficiency are also highly desired for searching for more efficient bioremediation catalysts.

Kinetic, spectroscopic, and structural studies of the dehalogenase have shown that catalysis proceeds by a multistep mechanism (Scheme 1),[1,17−30] in which the carboxylate group

[†] University of New Mexico.
[‡] University of Wisconsin.
[§] University of Minnesota.

(1) Scholten, J. D.; Chang, K.-H.; Babbitt, P. C.; Charest, H.; Sylvestre, M.; Dunaway-Mariano, D. *Science* **1991**, *253*, 182.
(2) Dunaway-Mariano, D.; Babbitt, P. C. *Biodegradation* **1994**, *5*, 259.
(3) Loffler, F.; Lingens, F.; Muller, R. *Biodegradation* **1995**, *6*, 203.
(4) Abramowicz, D. A. *Crit. Rev. Biotechnol*. **1990**, *10*, 241.
(5) Commandeur, L. C. M.; Parsons, J. R. *Biodegradation* **1990**, *1*, 207.
(6) Cannon, W. R.; Benkovic, S. J. *Biochemistry* **1998**, *273*, 26257.
(7) Bruice, T. C.; Lightstone, F. C. *Acc. Chem. Res*. **1999**, *32*, 127.
(8) Kollman, P. A.; Kuhn, B.; Perakyla, M. *J. Phys. Chem*. **2002**, *B106*, 1537.
(9) Warshel, A.; Aqvist, J.; Creighton, S. *Proc. Natl. Acad. Sci. U.S.A.* **1989**, *86*, 5820.
(10) Warshel, A. *Proc. Natl. Acad. Sci. U.S.A.* **1978**, *75*, 5250.
(11) Warshel, A. *J. Biol. Chem*. **1998**, *273*, 27035.
(12) Jencks, W. P. *Catalysis in Chemistry and Enzymology*; Dover: New York, 1986.
(13) Fersht, A. R.; *Enzyme Structure and Mechanism in Protine Science*; Freeman: New York, 1999.
(14) Villa, J.; Warshel, A. *J. Phys. Chem*. **2001**, *B105*, 7887.
(15) Benkovic, S. J.; Hammes-Schiffer, S. *Science* **2003**, *301*, 1196.
(16) Garcia-Viloca, M.; Gao, J.; Karplus, M.; Truhlar, D. G. *Science* **2004**, *303*, 186.
(17) Crooks, G. P.; Copley, S. D. *J. Am. Chem. Soc*. **1993**, *115*, 6422.
(18) Yang, G.; Liang, P.-H.; Dunaway-Mariano, D. *Biochemistry* **1994**, *33*, 8527.
(19) Liu, R.-Q.; Liang, P.-H.; Scholten, J.; Dunaway-Mariano, D. *J. Am. Chem. Soc*. **1995**, *117*, 5003.
(20) Crooks, G. P.; Xu, L.; Barkley, R. M.; Copley, S. D. *J. Am. Chem. Soc*. **1995**, *117*, 10791.
(21) Taylor, K. L.; Liu, R.-Q.; Liang, P.-H.; Price, J.; Dunaway-Mariano, D. *Biochemistry* **1995**, *34*, 13881.

Scheme 1. Proposed Mechanism of 4-CBA-CoA Dehalogenase Catalysis

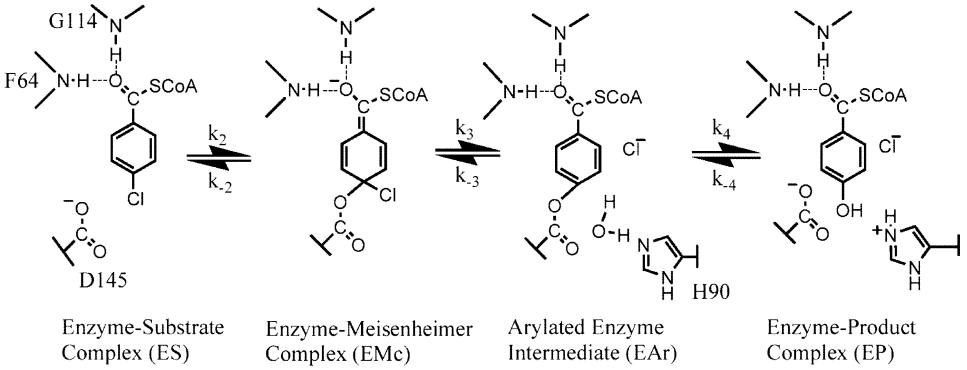

of active site Asp145 displaces the ring chloride of the bound substrate (ES complex), thereby forming an arylated enzyme intermediate (EAr). His90 base-catalyzed hydrolysis ensues, forming the 4-hydroxybenzoyl-CoA (4-HBA-CoA) product and regenerating the Asp145 nucleophile.

In this work, we concentrate on the aromatic substitution (S_NAr) step leading to a chemically stable intermediate EAr, to address the following question: does the reaction proceed via the active site stabilized, covalently bonded enzyme-Meisenheimer (EMc) intermediate pictured in Scheme 1? Nucleophilic substitution on an aromatic ring substituted with strong electron-withdrawing groups will proceed via an addition−elimination mechanism because the high-energy carbanionic reaction intermediate, or "Meisenheimer complex" (Mc), is stabilized by electron delocalization onto the electropositive ring-activating groups.[31] Because the thioester substituent of the 4-CBA-CoA reactant is not a powerful activator, it follows that ring activation is accomplished by the dehalogenase active site. The mechanism by which the dehalogenase performs this task has been the focal point of previous work.[23−25,27−29] Inspection of the active site structure (Figure 1) reveals that ring activation can be provided by two hydrogen bonds that exists between the substrate benzoyl carbonyl oxygen and the backbone amide NHs of Gly114 and Phe64, with potential enhancement from the positive pole of the helical dipole terminated at Gly114.[30] Ring polarization by this electron-withdrawing effect (the "pull") might be amplified by electron donation from the carboxylate oxygen of Asp145 at the C(4) position of the benzoyl group (the "push"). The electrostatic interactions lead to significant changes in charge distribution and bonding characteristics that are manifested in UV−VIS and Raman spectra of the bound ligand. The rearrangement of the π electrons in the benzoyl moiety is supported by the surrounding hydrophobic side chains of Phe64, Phe82, Trp89, and Trp137, also shown in Figure 1.

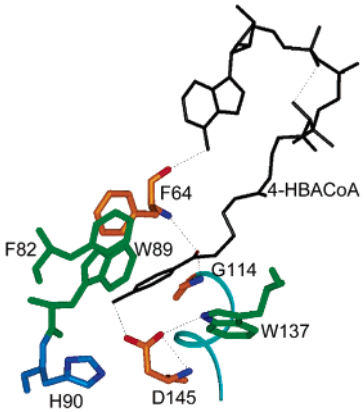

Figure 1. X-ray structure of the active site of the 4-HBA-CoA complex.

Although the potential for dehalogenase stabilization of an EMc complex is evident, this complex has neither been trapped nor detected during catalytic turnover of 4-CBA-CoA. Its possible existence has, however, been inferred from the measurement of the EAr population by rapid quenching[18,26,29] and from kinetic and spectroscopic studies of the reaction of the enzyme with alternate substrates having poor leaving groups at C(4) (viz. 4-fluoro- and 4-nitrobenzoyl-CoA).[21,23−25,28,29] Here, we use a theoretical approach to test the intermediacy of a stabilized EMc complex in dehalogenase-catalyzed 4-CBA-CoA dechlorination.

Thanks to the extensive structural and kinetic data available on the dehalogenase, several theoretical investigations have been reported. Lau and Bruice[32] carried out a molecular dynamics (MD) simulation of the active site dynamics of ES complex, using an empirical force field. It was observed that a carboxylate oxygen of Asp 145 is preferentially oriented to attack the C(4) of the benzoyl group. In addition, strong hydrogen bonding persisted between the benzoyl carbonyl group and the backbone amide NHs of Gly114 and Phe64, in strong support of the activation mechanism suggested by the experiments. Using Hartree−Fock (HF), density functional theory (DFT), and semiempirical PM3 methods, Zheng and Bruice[33] have also investigated a model S_NAr reaction between acetate and 4-Cl−Ph−CO−SMe in both the gas phase and solution. The PM3 method was found to be quite accurate when compared with the DFT results, an important prerequisite for the current study. However, the Mc was not found in HF and DFT calculations, although a very shallow well corresponding to the complex was

(22) Yang, G.; Liu, R.; Taylor, K. L.; Xiang, H.; Price, J.; Dunaway-Mariano, D. *Biochemistry* **1996**, *35*, 10879.
(23) Taylor, K. L.; Xiang, H.; Liu, R.-Q.; Yang, G.; Dunaway-Mariano, D. *Biochemistry* **1997**, *36*, 1349.
(24) Clarkson, J.; Tonge, P. J.; Taylor, K. L.; Dunaway-Mariano, D.; Carey, P. R. *Biochemistry* **1997**, *36*, 10192.
(25) Dong, J.; Xiang, H.; Luo, L.; Dunaway-Mariano, D.; Carey, P. R. *Biochemistry* **1999**, *38*, 4198.
(26) Zhang, W.; Wei, Y.; Luo, L.; Taylor, K. L.; Yang, G.; Dunaway-Mariano, D.; Benning, M. M.; Holden, H. M. *Biochemistry* **2001**, *40*, 13474.
(27) Luo, L.; Taylor, K. L.; Xiang, H.; Wei, Y.; Zhang, W.; Dunaway-Mariano, D. *Biochemistry* **2001**, *40*, 15684.
(28) Dong, J.; Carey, P. R.; Wei, Y.; Luo, L.; Lu, X.; Liu, R.-Q.; Dunaway-Mariano, D. *Biochemistry* **2002**, *41*, 7453.
(29) Dong, J.; Lu, X.; Wei, Y.; Luo, L.; Dunaway-Mariano, D.; Carey, P. R. *Biochemistry* **2003**, *42*, 9482.
(30) Benning, M. M.; Taylor, K. L.; Liu, R.-Q.; Yang, G.; Xiang, H.; Wesenberg, G.; Dunaway-Mariano, D.; Holden, H. M. *Biochemistry* **1996**, *35*, 8103.
(31) Miller, J. *Aromatic Nucleophilic Substitution*; Elsevier: Amsterdam, 1968.
(32) Lau, E. Y.; Bruice, T. C. *Proc. Natl. Acad. Sci. U.S.A.* **2001**, *98*, 9527.
(33) Zheng, Y.-J.; Bruice, T. C. *J. Am. Chem. Soc.* **1997**, *119*, 3868.

located in the PM3 potential energy surface. This is not entirely surprising, because there is no ring electron-withdrawing group present in the model. On the other hand, stable Mc has been obtained in HF and DFT optimizations of fluoro/nitro-substituted intermediates by Dong et al.[28] In addition, Zheng and Bruice have also investigated the solvent effect using a polarizable continuum model (PCM) of aqueous solution.[33] Apparently, a polar solvent significantly increases the reaction barrier by preferentially stabilizing the reactant and product. This observation provides a rationale for the hydrophobic active site residues surrounding the benzene ring.

Despite the considerable insight gained from these theoretical studies, they have either ignored the enzymatic environment or failed to incorporate bond forming/cleavage. In this work, we report a combined quantum mechanical/molecular mechanical (QM/MM) study of the S_NAr step of the dechlorination reaction catalyzed by the 4-CBA-CoA dehalogenase. In particular, we describe the active site dynamics and the potential of mean force (PMF) along the reaction coordinate for both the wild-type (WT) enzyme and the G113A mutant, which lacks full ring polarization capability. Our results indicate that the EMc is indeed formed during the substitution reaction as an intermediate, stabilized by strong electrostatic forces in the active site. In addition, the formation of the EMc is the rate-determining step, thus resolving a long-standing uncertainty in the kinetic model. A preliminary communication of our work has been published recently,[34] but the results and insights thus derived are significantly expanded. This paper is organized as follows. Details of the computation are outlined in the following section (section II). The calculated results are presented and discussed in section III. The final section (section IV) summarizes our conclusions.

II. Computational Methods

To advance our understanding of the mechanism of the S_NAr reaction catalyzed by the 4-CBA-CoA dehalogenase, the theoretical model has to not only incorporate in the simulation a large portion of the solvated enzyme but also be able to handle bond-forming and -breaking processes. The QM/MM approach[35−38] is ideally suited for this purpose. The strategy is to partition the system into a QM region and a classical MM region. The QM region includes the reacting species and some other moieties that are expected to significantly impact the reaction, while the surrounding MM region provides a realistic reaction field. A force field approach is sufficient for describing the MM atoms as their thermal motion is largely near their equilibria. On the other hand, a quantum description of the potential energy surface for the QM atoms is necessary because of their reactive nature. The QM/MM approach synthesizes the generality of the QM models and the efficiency of MM force fields, and numerous studies have demonstrated that it is an effective method to characterize enzymatic reactions.[8,39−41] The computational protocol is similar to an earlier work on the haloalkane dehalogenase catalyzed reactions.[42]

The calculations reported in this work have been carried out using the CHARMM suite of molecular simulation programs.[43] For the WT enzyme, the starting geometry was modified from the high-resolution structure of the EP complex (Protein Data Bank code 1NZY)[30] by replacing the hydroxyl O atom in 4-HBA with Cl. Two subunits (A and B) were needed as several residues of subunit B are essential in stabilizing the phosphoryl groups of the CoA portion of the substrate and in preventing solvent water from entering the active site to perturb the hydrophobic environment surrounding the benzene ring.[30] The X-ray structure indicates that a phosphoryl group in CoA is missing in the crystal.[30] However, its inclusion in the simulation was not attempted because this group is exposed to solvent and quite far from the active site. Moreover, kinetic studies have shown that k_{cat} is not impacted by removal of the phosphoryl group from the substrate.[27] For the G113A mutant, a hydrogen atom of the Gly residue was replaced by a methyl group, followed by a short energy minimization to remove bad contacts. To simulate the physiological environment, both the WT and G113A mutant ES complexes were solvated in a 25 Å radius sphere of TIP3P water[44] using Cl as the origin. Solvation with a larger (30 Å radius) water sphere was tested and found to yield qualitatively similar results. Those bulk waters having an oxygen atom within 2.8 Å of a heavy atom or crystallographic water were deleted. A further 30 ps MD simulation was performed for bulk waters with the protein atoms and crystallographic waters fixed. This process was repeated several times with randomly rotated water spheres to make sure that there was no significant cavity in the solvent.

To minimize the computational costs, stochastic boundary conditions[45,46] were imposed, where the system was partitioned into three regions: the reaction region, the buffer region, and the reservoir region. A sphere of 22 Å radius centered at the Cl atom was used for the reaction zone, which was treated with Newtonian dynamics. Outside of the solvation sphere of 25 Å, the protein residues and all of waters were deleted. Atoms in the buffer zone (22−25 Å from the Cl atom) are subjected to Langevin dynamics, in which friction coefficients of 80 ps^{-1} were used for both protein atoms and waters. The atoms in the buffer region were further restrained with harmonic force fields to maintain the crystal structure, with the corresponding force constants gradually scaled to zero at the reaction zone boundary. The final size of the WT system contains 7473 atoms, including 88 substrate atoms, and 1122 water molecules. To account for the long-range solvent effect, a simple charge-scaling approach[47] was used. To that end, the partial charges on the charged residues exposed to the solvent were scaled according to classical Poisson−Boltzmann calculations. Such a procedure was invoked to avoid artificial structural changes and overpolarization of the QM wave function due to the small number of explicit solvent molecules included in stochastic boundary simulations. Tests show, however, that the charge-scaling procedure does not quantitatively change the results.

The atoms in the MM region are governed by the CHARMM22 all atom force field for protein.[48] The MM parameters of the CoA part of the substrate were adopted from previous work.[49] The QM region consists of 25 atoms in the Asp145 side chain and the benzoyl group of the 4-CBA-CoA substrate. Ideally, the QM region should be treated with *ab initio* or density functional theory (DFT) methods. However, the latter is still too expensive for MD simulations in which millions of QM calls are need. Most of the results reported in this work were

(34) Xu, D.; Guo, H.; Gao, J.; Cui, Q. *Chem. Commun*. **2004**, 892.
(35) Warshel, A.; Levitt, M. *J. Mol. Biol*. **1976**, *103*, 227.
(36) Singh, U. C.; Kollman, P. A. *J. Comput. Chem*. **1986**, *7*, 718.
(37) Field, M. J.; Bash, P. A.; Karplus, M. *J. Comput. Chem*. **1990**, *11*, 700.
(38) Gao, J.; Amara, P.; Alhambra, C.; Field, M. J. *J. Phys. Chem*. **1998**, *102 A*, 4714.
(39) Gao, J. *Acc. Chem. Res*. **1996**, *29*, 298.
(40) Monard, G.; Merz, K. M., Jr. *Acc. Chem. Res*. **1999**, *32*, 904.
(41) Cui, Q.; Karplus, M. *Adv. Protein Chem*. **2003**, *66*, 315.
(42) Devi-Kesavan, L. S.; Gao, J. *J. Am. Chem. Soc*. **2003**, *125*, 1532.
(43) Brooks, B. R.; Bruccoleri, R. E.; Olafson, B. D.; States, D. J.; Swaminathan, S.; Karplus, M. *J. Comput. Chem*. **1983**, *4*, 187.
(44) Jorgensen, W. L.; Chandrasekhar, J.; Madura, J. D.; Impey, R. W.; Klein, M. L. *J. Chem. Phys*. **1983**, *79*, 926.
(45) Brooks, C. L., III; Karplus, M. *J. Chem. Phys*. **1983**, *79*, 6312.
(46) Brooks, C. L., III; Karplus, M. *J. Mol. Biol*. **1989**, *208*, 159.
(47) Simonson, T.; Archontis, G.; Karplus, M. *J. Phys. Chem. B* **1997**, *101*, 8349.
(48) MacKerell, A. D. Jr., Bashford, D.; Bellott, M.; Dunbrack, R. L. Jr., Evanseck, J. D.; Field, M. J.; Fischer, S.; Gao, J.; Guo, H.; Ha, S.; Joseph-McCarthy, D.; Kuchnir, L.; Kuczera, K.; Lau, F. T. K.; Mattos, C.; Michnick, S.; Ngo, T.; Nguyen, D. T.; Prodhom, B.; Reiher, W. E., III; Roux, B.; Schlenkrich, M.; Smith, J. C.; Stote, R.; Straub, J.; Watanabe, M.; Wiorkiewicz-Kuczera, J.; Yin, D.; Karplus, M. *J. Phys. Chem*. **1998**, *B102*, 3586.
(49) Poulsen, T. D.; Garcia-Viloca, M.; Gao, J.; Truhlar, D. G. *J. Phys. Chem*. **2003**, *B107*, 9567.

Scheme 2. Atomic Definitions

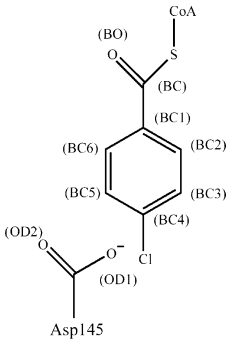

obtained using the semiempirical PM3 method for the QM region, while some selected single point calculations with HF are also included. Fortunately, earlier theoretical work on a model system analogous to the enzymatic reaction has extensively examined the performance of the PM3 method in this system and found it correlating closely with results at the B3LYP/6-311+G** level of theory.[33] It thus provides a sound basis for the semiempirical treatment of the S_NAr reaction catalyzed by the enzyme. In the PM3/CHARMM simulations, the interface between QM and MM regions, namely C_α of Asp145 and C_β of the mercaptoethylamine part of the CoA, was treated using the generalized hybrid orbital (GHO) method,[38] with standard van der Waals parameters of the CHARMM22 force field.

The putative reaction coordinate for the S_NAr reaction is defined as $R_\phi = R_{BC4-Cl} - R_{OD1-BC4}$ (see Scheme 2 for atom definitions). The energy of the reaction path was determined along the reaction coordinate by using the adiabatic mapping method, in which all coordinates except R_ϕ are optimized to minimize the total energy. The configurations generated in a R_ϕ grid were later used as initial conditions in the PMF calculations.

The MD calculations were carried out with a time step of 1 fs and the SHAKE algorithm[50] was used to maintain the covalent bonding involving H atoms. A nonbonded cutoff of 12 Å was employed. All calculations were initiated with an equilibration period in which the temperature was slowly raised to 300 K, at which the final data collection was performed. For the active site dynamics, the system was allowed to equilibrate for 250 ps and the results were collected for 1.0 ns. In the potential of mean force (PMF) simulations, the system at each window was first equilibrated for 50 ps, followed by data collection for an additional 50 ps.

The PMF for the catalyzed S_NAr reaction was determined by umbrella sampling[51] along the reaction coordinate R_ϕ. The PMF as a function of the reaction coordinate is related to the relative probability density $g(R_\phi)$ and can be written as $\Delta G(R_\phi) = -k_BT \ln g(R_\phi) + C$,[51] where k_B is the Boltzmann constant and C is a constant. To facilitate efficient sampling, the reaction coordinate was constrained with harmonic biasing potentials in several windows. The final PMF was obtained using the weighted histogram analysis method (WHAM).[52] The PMF accounts for protein fluctuation and entropic effects and is essential for a more reliable estimate of the rate constant using the transition rate theory. In this work, we ignored the influence of the transmission coefficient, which is assumed to be unity, as suggested by many previous studies of reactions involving heavy atoms.[14,53,54]

III. Results

1. Dynamics of ES Complexes of WT Enzyme and G113A Mutant. We first discuss the active site dynamics for the Michaelis (ES) complexes of the WT enzyme and the G113A mutant at 300 K, obtained from the 1 ns QM/MM MD simulations. The initial structures were modified from the dehalogenase-4-HBA-CoA (EP) crystal structure, following the protocol discussed in the previous section. During the 1.0 ns of MD production run, the structure for the WT dehalogenase was reasonably stable, as evidenced by the relatively small (0.95 Å) root-mean-square deviation (rmsd) of the main chain atoms. A similar level of fluctuation (rmsd = 0.93 Å) was also observed for the mutant. The interactions of the 4-CBA-CoA with both the WT and mutant enzyme remain intact throughout the simulation, although the part of CoA exposed to the solvent experiences larger fluctuations than the regions embedded in the enzyme. Throughout the simulation, persistent hydrogen bonding is seen between the adenine AN1 and the backbone amide NH of Leu66 and between adenine AN6 and backbone carbonyl O of Phe64, consistent with the X-ray structure.

Compared with the X-ray structure of the WT EP complex,[30] however, the position and orientation of Asp145 of the enzyme−4-CBA-CoA (ES) complex are significantly different. One of the most important changes observed is the interaction between the OD1 atom of Asp145 and the NE1-H group of the Trp137 side chain. In the crystal structure of the EP complex, the distance of OD1···NE1 is 2.88 Å. As a result, it was believed that the hydrogen bond indicated is responsible for the alignment of the reactants.[30] However, our simulations indicate that the average OD1···NE1 distance is 4.7 ± 0.5 Å in the ES complex, suggesting that the hydrogen bond is either very weak or nonexistent. The replacement of Gly113 to Ala appears to have little impact on the above picture. The reason for the change in Asp145 orientation in the ES vs the EP complex appears to be two-fold. First, the Cl atom at the BC4 position of the substrate does not contribute to the positioning of the Asp145 OD2 as did the H-bond formed with the BC4 OH of the 4-HBA-CoA ligand. Second, the Asp145 carboxylate group must assume a different orientation to accommodate the larger Cl substituent. A snapshot of the active site structure of the ES complex is displayed in Figure 2.

An interesting observation from our simulations of the WT complex is that the OD1 and OD2 atoms may exchange positions with each other, as shown in Figure 3, wherein the distances between BC4 and OD1/OD2 are plotted. The switch, although very fast, occurs only once during the 1 ns simulation, thus indicating a double-well, separated by a significant barrier, for the interconversion of carboxylate conformers. Conformational switching is also observed in the mutant simulation. Because of the equivalency of the two oxygen atoms of the carboxylate group, we will hereafter denote the one closest to BC4 as OD1.

The prevailing orientation of the Asp145 in the WT ES complex has an average OD1−BC4 distance of 3.4 ± 0.2 Å, which is much shorter than the OD2−BC4 distance (4.7 ± 0.3 Å). This is in accord with the earlier MD study by Lau and Bruice based on an MM force field (3.26 ± 0.2 and 3.67 ± 0.3 Å).[32] While the OD1−BC4 distance is similar to the value that these authors found in their simulations, OD2 appears to be farther from BC4 in our study. The differences might be due to the empirical force field used in the earlier work. The OD1−BC4−BC3 and OD1−BC4−BC5 angles are 107° ± 11° and 96° ± 12°, slightly larger than the values obtained by Lau and

(50) Ryckaert, J. P.; Ciccotti, G.; Berendsen, H. J. *J. Comput. Phys.* **1977**, *23*, 327.
(51) Torrie, G. M.; Valleau, J. P. *J. Comput. Phys.* **1977**, *23*, 187.
(52) Kumar, S.; Bouzida, D.; Swendsen, R. H.; Kollman, P. A.; Rosenberg, J. M. *J. Comput. Chem.* **1992**, *13*, 1011.
(53) Neria, E.; Karplus, M. *Chem. Phys. Lett.* **1997**, *267*, 23.
(54) Nam, K.; Prat-Resina, X.; Garcia-Viloca, M.; Devi-Kesavan, L. S.; Gao, J. *J. Am. Chem. Soc.* **2004**, *126*, 1369.

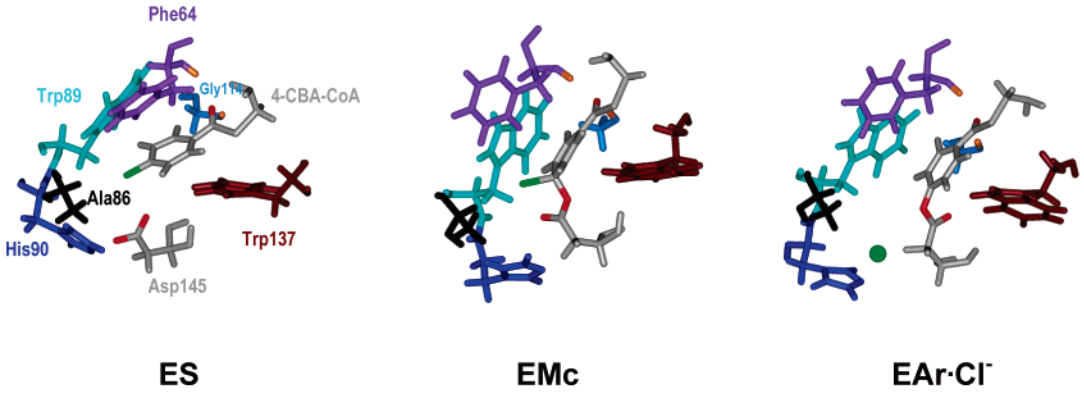

Figure 2. Snapshots of the ES, EMc, and EAr·Cl^- complexes.

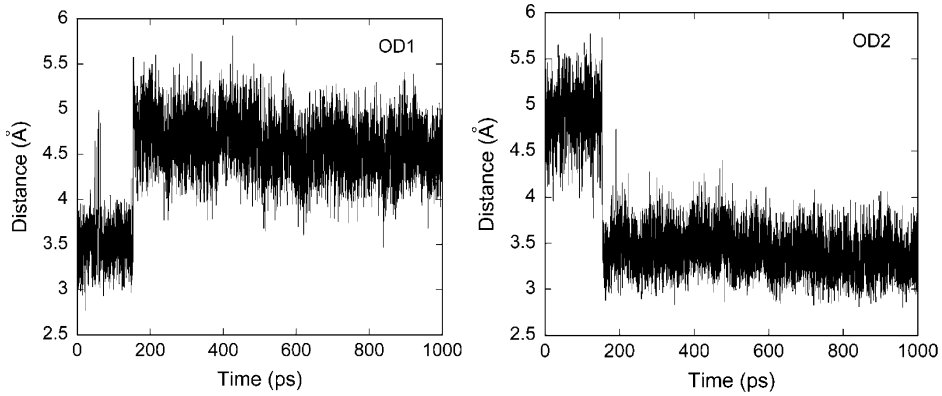

Figure 3. OD1−BC4 and OD2−BC4 distances obtained from MD simulation of the ES complex.

Bruice (97° ± 12° and 82° ± 10°).[32] They are close to those observed by Zheng and Bruice for the transition state configuration of the gas-phase model reaction.[33] The OD2 atom forms a hydrogen bond with the backbone amide NH of Thr146 at an OD2−H distance of 2.5 ± 0.3 Å, while the OD1 is close to the backbone amide NH of Asp145 at an OD1−H distance of 2.6 ± 0.3 Å. Note that these hydrogen bonds are not necessarily optimal, because the N−H−O angles are less than 180°. In the G113A mutant, the situation is similar. For instance, the OD1−BC4 and OD2−BC4 distances are 3.4 ± 0.3 and 4.7 ± 0.4 Å, respectively. The hydrogen bonds with backbone amide NHs are also present. Overall, the mutation at the 113 position has only limited impact on the orientation of the nucleophile.

The key active site residue His90 serves as a solvent barrier[30] and a general base in the hydrolysis step.[26] In agreement with the crystal structure, a hydrogen bond exists between ND1−HD1 and the backbone C═O of Ala86 (O···H distance = 2.0 ± 0.2 Å in the WT ES complex). The CA−CB−CG−CD2 dihedral angle of the imidazole ring of −91° ± 11° is close to the experimental value of −88.5° [30] and maintained throughout the simulation, as depicted in Figure 4. (The atom labels follow the CHARMM topological file.) These observations are consistent with previous simulation results[32] and are not significantly perturbed by the mutation at the 113 position.

Concurring with earlier simulations,[32] our results show persistent cooperative hydrogen bonding[55] between the benzoyl carbonyl oxygen and the backbone amide NHs of Gly114 and Phe64 of the WT ES complex. The hydrogen bond with the NH of Gly114 appears to be strong, as is evidenced by an

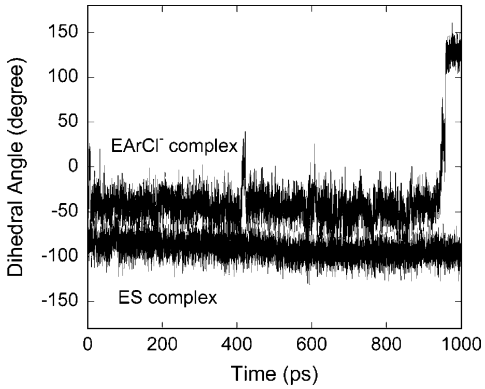

Figure 4. CA−CB−CG−CD2 dihedral angle of the His90 residue obtained from MD simulations of the ES and EAr·Cl^- complexes.

O···H distance of 2.1 ± 0.2 Å, which is likely aided by the terminal dipole of the α-helix.[56] On the other hand, the hydrogen bond with Phe64 is weaker and more floppy with an O···H distance of 2.8 ± 0.6 Å. This observation is consistent with the experimental data that indicate that Gly114 makes a larger contribution to reactant binding and transition-state stabilization than does Phe64.[27]

The Gly114 position is the center of the conserved sequence motif GGG. The absence of space-requiring side chains at the α-helix terminus might facilitate interaction with the reactant. Site-directed mutagenesis studies have shown that amino acid replacements made at or near the N-terminus are detrimental to catalysis. For example, the replacement of the C_α-H with C_α-CH_3 in the G113 is known to reduce k_{cat} by 120-fold.[27] The

(55) Guo, H.; Salahub, D. R. *Angew. Chim. Intl. Ed.* **1998**, *37*, 2985.

(56) Hol, W. G. *Prog. Biophys. Mol. Biol.* **1985**, *45*, 149.

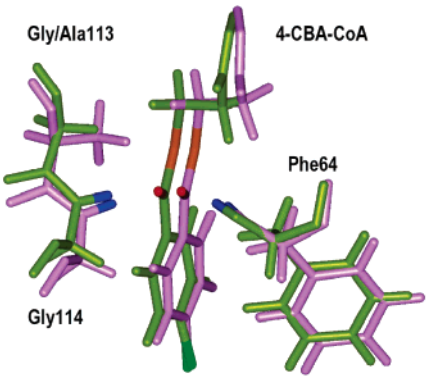

Figure 5. Overlay of active site residues surrounding the substrate benzoyl carbonyl of the wild-type enzyme (green) and the G113A mutant (purple).

reduction in rate is attributed to the S_NAr partial reaction, because the formation of the EAr is rate-limiting in the mutant. In addition, the Raman spectrum of the G113A mutant indicated a reduction of the C═O polarization,[29] presumably due to the weakening of the electropositive force in the "oxyanion hole" formed by the backbone amide NH groups.

Indeed, the simulation of the G113A mutant ES complex shows that the hydrogen bond between the benzoyl carbonyl oxygen and the backbone amide NH of Gly114 is significantly elongated and more floppy. The hydrogen bond (O···H) distance of 2.7 ± 0.4 Å can be compared with that in the WT ES complex (2.1 ± 0.3 Å). On the other hand, the corresponding O···H distance for Phe64 is shortened to 2.2 ± 0.3 Å from 2.8 ± 0.6 Å in the WT complex. The structure changes are apparently due to the steric effect of the more bulky methyl side chain, which pushes the substrate away from the α-helix terminated at the 114 position. An overlay of some nearby residues of the WT and mutant "oxyanion hole" is shown in Figure 5, which clearly shows the displacement of the substrate in the mutant enzyme. Given that the hydrogen bond with the backbone amide of Gly114 plays the dominating role in the "oxyanion hole", its weakening is expected to lead to substantial reduced stabilization of the transition state and the EMc intermediate leading to the EAr intermediate.

Consistent with reduced hydrogen-bond interaction with substrate and product ligands in the G113A mutant is the observation that mutant binding of the substrate analogue 4-methylbenzoyl-CoA (4-MeBA-CoA) and the product 4-HBA-CoA is considerably weaker (4-HBA-CoA $K_d = 16 \pm 2$ μM; 4-MeBA-CoA $K_d = 25 \pm 4$ μM) than that observed for the wild-type enzyme (4-HBA-CoA $K_d = 0.6 \pm 0.2$ μM; 4-MeBA-CoA $K_d = 1.6 \pm 0.2$ μM).[57] Similarly, K_m for the G113A mutant is also increased by a factor of 4.[29] As will be discussed below, the role of hydrogen-bond interaction intensifies in the transition state and especially in the EMc intermediate, and therefore reduction in the hydrogen-bond interaction has a larger impact on these internal states than it does on the ES and EP complexes.

As illustrated in Scheme 1, a water molecule is needed for the hydrolysis of the EAr intermediate. However, it is still not clear whether the water is present in the active site before the substrate binding. Lau and Bruice reported that a H_2O molecule can diffuse into the active site on a nanosecond time frame.[32] However, our simulations could not reproduce their observation.

(57) Wei, Y. Dissecting and Expending Catalysis in 4-Chlorobenzoyl-CoA Dehalogenase. Ph.D. Thesis, University of New Mexico, 2003.

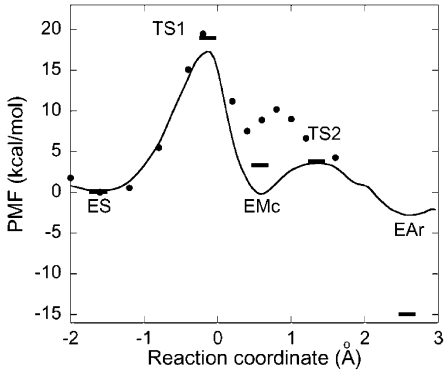

Figure 6. PMF of the S_NAr reaction catalyzed by the wide-type 4-CBA-CoA dehalogenase. The filled circles are single point HF/MM results along the reaction coordinate, and the bars are free energies of a model gas-phase reaction between acetate ion and 4-Cl−Ph−CO−SMe.[38]

2. Potential of Mean Force for Wild-Type Enzyme. To provide mechanistic insights into the enzymatic S_NAr reaction, we have computed the QM/MM PMFs for both the WT enzyme and the G113A mutant along the putative reaction coordinate R_ϕ. In particular, we divided the coordinate space into 27 separate windows and used a harmonic biasing potential energy in each window. The force constant of the biasing potential was between 50 and 80 kcal/mol Å^2. The initial configuration for the MD simulation in each window was adopted from the minimal energy configuration determined by adiabatic mapping. A 50 ps MD propagation was found sufficient to converge the PMFs.

The PMF for the S_NAr dechlorination reaction catalyzed by the WT 4-CBA-CoA dehalogenase is shown in Figure 6. For comparison, we also include in the figure the PM3 free energies obtained by Zheng and Bruice[33] for a model gas-phase S_NAr reaction between acetate ion and 4-Cl−Ph−CO−SMe. The zero is arbitrarily chosen at the potential minimum corresponding to the ES complex ($R_\phi = -1.6$ Å). It is interesting to note the existence of the middle well at $R_\phi = 0.6$ Å corresponding to the EMc complex. The covalent Cl−BC4 and OD1−BC4 bond lengths are 1.98 and 1.38 Å in the minimal energy configuration at $R_\phi = 0.6$ Å, very close to the nominal Mc found in an earlier PM3 study of the gas-phase analogue (1.976 and 1.423 Å).[33] The appearance of this potential minimum is attributed to the stabilization resulting from strong hydrogen-bonding interaction between the backbone amide NHs of Gly114 and Phe64 and the charged oxygen of the enethiolate anion. Indeed, the O−H distances, retrieved from the PMF calculation in the EMc window, are shortened substantially near EMc (2.0 ± 0.1 Å for Gly114 and 2.0 ± 0.2 Å for Phe64), indicating that stronger interactions take place near the transition state. To further ascertain the accuracy of the model, we have carried out single point HF/MM calculations along the reaction path using the 6-31+G** basis set. The results (filled circles in Figure 6) are consistent with the presence of a transient EMc intermediate, although it appears to be higher in energy. The structure of the EMc complex is depicted in Figure 2.

A detailed analysis along the reaction coordinate provides strong evidence in support for stabilization of the transition state and EMc intermediate by the "oxyanion hole" conserved throughout the enoyl-CoA (crotonase/isomerase) enzyme superfamily.[58] In addition to the electrophilic interactions with the benzoyl carbonyl, Figure 7 illustrates substantial charge

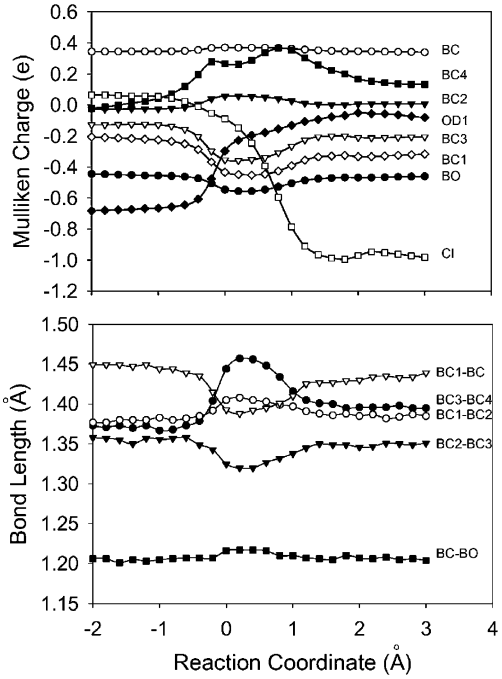

Figure 7. Mulliken charges and bond lengths of selected benzoyl atoms along the reaction path. Due to symmetry, some benzene atoms are not shown.

migration and structure distortion in the benzoyl moiety. Such changes have been inferred from the UV and Raman spectra of the enzyme-ligand complexes.[21,24,29] Ring polarization is an essential prelude to attack by the charged nucleophile. In the upper panel, the Mulliken charges of selected benzoyl atoms along the reaction path are plotted. In addition to the monotonic changes in the OD1 and Cl charges, there is significant charge migration from the BC4 position of the benzene ring to the carbonyl. Most conspicuously, there is negative charge buildup at the BO, BC1, and BC3/BC5 in the vicinity of the EMc (R_ϕ = 0.6 Å), whereas additional positive charges are found at BC4 and BC2/BC6. Concomitantly, the BC1−BC bond distance is shortened, while the BC−BO bond length is elongated. Within the "benzene" ring, which maintains a near planar structure, the formation of the EMc results in the shortening of the BC2−BC3/BC5−BC6 bonds and the elongation of the BC1−BC2/BC1−BC6 as well as BC3−BC4/BC4−BC5 bonds. The single/double bond alternating quinone-like structure is similar to previous theoretical predictions of the Mc structure.[28,33] As the EAr complex is formed, the aromaticity in the benzoyl moiety is largely restored. It is clear from Figure 7 that the charge redistribution and structural distortion are the greatest near R_ϕ = 0.6 Å, which is suggestive of the greater concentration of charge at the oxygen atom in the EMc relative to its flanking transition states.

It is interesting to note that the free energy barrier for the uncatalyzed S_NAr reaction in aqueous solution is estimated to be 37 kcal/mol.[33] The ~20 kcal/mol reduction in the energy barrier implies significant stabilization of the transition state by the enzyme active site. As discussed above, this is realized by the "oxyanion hole" formed by the backbone amide NHs. Thus, this system can be considered as a prime example of the "solvent substitution" effect,[9] in which a preorganized electrostatic field exerted by the active site helps to lower the reaction barrier relative the corresponding solution reaction.

The contribution of the hydrogen-bond formation with Gly114 and Phe64 to ground state (ES) and the rate-limiting transition state (TS1) of the WT enzyme can be measured experimentally. In an earlier study, the contribution of the hydrogen-bond interactions to the stabilization of the rate-limiting transition state was determined to be −4.9 kcal/mol.[27] In the present work, the inhibition constant of 4-chlorobenzyl-CoA ($K_i = 700 \pm 80$ μM) was measured using the steady-state kinetic techniques described in ref 27 to define the dissociation constants for the corresponding enzyme−inhibitor complex. (The K_i value of 55 μM for 4-CBA-CoA reported in ref 27 was found to be incorrect.) Owing to the absence of the benzoyl C=O, the 4-chlorobenzyl-CoA ligand cannot engage in hydrogen-bond interaction with the oxyanion hole. The K_d of the dehalogenase−substrate complex is ~4 μM.[17] The ground-state stabilization ($\Delta\Delta G_{ES} = -RT \ln K_d^{inhibitor}/K_d^{substrate}$) is therefore −3.0 kcal/mol for the ES complex. The hydrogen-bond contribution to the stabilization of the transition state leading to EMc relative to the ES complex is thus estimated to be 1.9 kcal/mol.

The simulation also shows that chloride ion expulsion from EMc proceeds over a small energy barrier (3.8 kcal/mol) and is thus essentially spontaneous. This is not true, however, for the dehalogenase-catalyzed reaction of 4-FBA-CoA, where the energy barrier for fluoride expulsion is estimated from the rate constant for the catalyzed reaction (1×10^{-5} s^{-1}) to be 24 kcal/mol.

Finally, the EAr complex, which includes the chloride ion, is destabilized by the enzyme by ~12 kcal/mol relative to the gas-phase model. There may be two reasons for the seemingly large difference. First, the reaction coordinate defined here is for the S_NAr reaction, which is not suited for finding the optimal site for the chloride ion product in the binding pocket. This point will be addressed in more detail below. Second, the active site of 4-CBA-CoA dehalogenase is very tight and has no apparent polar residues to bind the bulky Cl^- ion. This is in sharp contrast to the haloalkane dehalogenases, where two tryptophan residues stabilize the halide ion leaving group.[42,59,60] In the present case, the origin of the rate-limiting barrier is due to the destruction of the aromatic conjugation in the reactant state, which is assisted by the push−pull mechanism discussed above. The recovery of aromaticity provides the driving force for the C−Cl bond cleavage.

3. Kinetic Model. The PMF for the S_NAr reaction catalyzed by the WT dehalogenase obtained from the QM/MM simulations indicates that the formation of EMc from ES is the rate-limiting step. The microscopic rate constants can be calculated from the simulated free energy profile according to transition state theory at T = 300 K:

$$k = \frac{k_B T}{h} \exp(-\Delta G^*/RT)$$

where k_B, h, and R are Boltzmann, Planck, and gas constants, respectively, and ΔG^* is the activation free energy. The resulting rate constants (defined in Scheme 1) are k_2 = 1.3 s^{-1}, k_{-2} =

(58) Holden, H. M.; Benning, M. M.; Haller, T.; Gerlt, J. A. *Acc. Chem. Res.* **2001**, *34*, 145.
(59) Verschueren, K. H. G.; Seljee, F.; Rozeboom, H. J.; Kalk, K. H.; Dijkstra, B. W. *Nature* **1993**, *363*, 693.
(60) Lightstone, F. C.; Zheng, Y.-J.; Bruice, T. C. *J. Am. Chem. Soc.* **1998**, *120*, 5611.

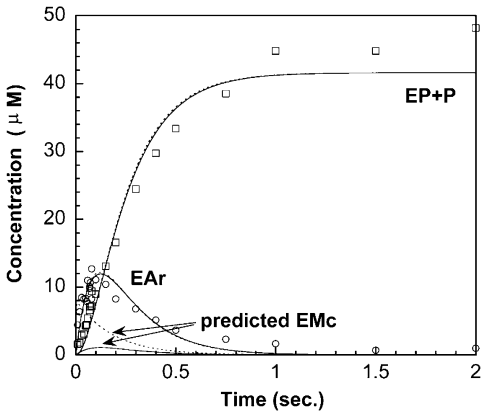

Figure 8. Fitting of single turnover time course data (scattered points). Solid and dashed curves were simulated using two kinetic models described in the text.

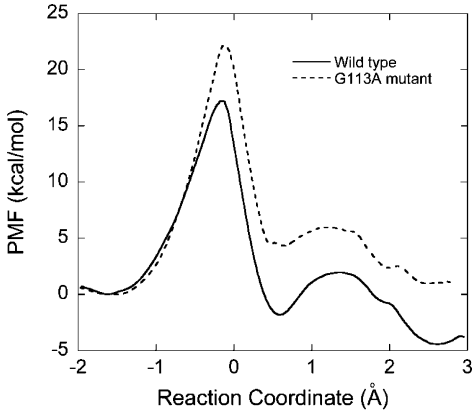

Figure 9. Comparison of the PMFs for the S_NAr reaction catalyzed by the wild-type enzyme and the G113A mutant. Both PMFs are related to their corresponding ES energies, which are set to zero.

0.91 s^{-1}, $k_3 = 1.0 \times 10^{10}$ s^{-1}, and $k_{-3} = 1.3 \times 10^8$ s^{-1}. The large $k_{\pm 3}$ values stem from the small barrier height of the second transition state (TS2) in Figure 6, indicating rapid equilibration between EMc and EAr. This is consistent with an earlier ab initio study of the S_NAr reaction of 1-chloro-2,4-dinitrobenzene catalyzed by glutathione S-transferases,[61] in which a small barrier between the Mc and product was as also found.

The calculated rate constants were used as initial input, along with the kinetic model shown in Scheme 1 and the computer program KINSIM,[62] to fit, by rate constant iteration, the single turnover time courses for ES, EAr, and EP. The time courses shown in Figure 8 were measured by reacting 52 μM 4-CBA-CoA and 115 μM dehalogenase at pH 7.5 and 25 °C in a rapid quench instrument, followed byproduct analysis, according to the procedures reported in ref 28. The kinetic solution obtained, and shown in Figure 8 (solid lines), defined $k_2 = 6.0$ s^{-1}, $k_{-2} = 4.3$ s^{-1}, $k_3 = 1 \times 10^{10}$ s^{-1}, $k_{-3} = 1.3 \times 10^8$ s^{-1}, $k_4 = 12$ s^{-1}, and $k_{-4} = 0.01$ s^{-1}. Provided that the k_3/k_{-3} ratio was maintained at ~100 and $k_3 > 100$ s^{-1}, the fit was insensitive to the exact value of k_3 used, because the EMc dechlorination is fast relative to EMc formation. The essentially identical set of simulated curves, shown as dashed lines in Figure 8, were obtained using the assumptions made in an earlier kinetic model, i.e., EMc formation is rate-limiting.[26,28] In this instance, we obtained $k_2 = 200$ s^{-1}, $k_{-2} = 1000$ s^{-1}, $k_3 = 35$ s^{-1}, $k_{-3} = 0.001$ s^{-1}, $k_4 = 12$ s^{-1}, and $k_{-4} = 0.01$ s^{-1}.[57] The near identical curves for EP + P and EAr populations clearly indicate that the single turnover time courses for ES, EAr, and EP cannot distinguish between rate-limiting EMc formation and rate-limiting EAr formation. Yet the QM/MM simulations can, and they predict rate-limiting EMc formation, with rate constants that are consistent with the experimental time course data. Because the barrier for conversion of EMc to EAr is small, EMc is not a kinetically significant intermediate, despite the amount of stabilization it receives as it forms from the ES complex. Interestingly, the new kinetic model reveals a much smaller population of EMc than the previous model, consistent with the futility in detecting the intermediate.

4. Potential of Mean Force for the G113A Mutant. To further elucidate the role of the "oxyanion hole" in the catalysis, we have computed the PMF of the S_NAr reaction catalyzed by the G113A mutant. As discussed above, the introduction of a methyl side chain to residue 113 results in a significant steric effect that pushes the substrate away from the α-helix and reduces the electropositive force acting on the benzoyl carbonyl. These changes are reflected in the free energy profile of the reaction. From Figure 9, it can be seen that the mutation results in an increase of barrier height at the first transition state (TS1) by 5.0 kcal/mol. The EMc intermediate is also destabilized by about 6.4 kcal/mol.

The calculated energy increase at TS1 is comparable with the experimental observation of a 120-fold reduction of k_{cat} (0.005 s^{-1}),[27] which corresponds to a free energy change of 2.9 kcal/mol. However, it is probably more meaningful to compare the change in the single turnover rate. The single turnover rate for the EAr formation is 25 s^{-1} in the WT enzyme[29] and 0.005 s^{-1} for the EP formation in the G113A mutant.[29] Since EAr does not accumulate in a single turnover reaction of the mutant, the formation of EAr is rate-limiting. Thus, this 5000-fold change in the single turnover rate corresponds to a 5.1 kcal/mol increase of the free energy barrier, in excellent agreement with the theoretical prediction.

There is little doubt that the steric effect of the 113 side chain contributes to the increased barrier height at TS1 by disrupting the "oxyanion hole". However, it is much more difficult to separate the effect into the individual contributions by the two hydrogen bonds, the α-helix, and the pure steric effect. All may have contributed. What is clear from the PMF of the mutant is that the combined influence of these factors differentially destabilizes the rate-limiting transition state, the metastable EMc intermediate, and the ES complex.

5. Dynamics of EAr·Cl^-. An important question regarding the dehalogenase reaction remains, namely, what happens to the chloride ion after its expulsion from the benzoyl ring? In particular, is there a binding site for the product ion? And when and how would the ion depart from the active site? Unlike haloalkane dehalogenase, where two Trp residues are used to bind the chloride ion,[59] there is no apparent halide ion binding residue in the 4-CBA-CoA dehalogenase active site. To elucidate the fate of the ion, we carried out a nanosecond time scale MD simulation of the EAr·Cl^- complex of the WT enzyme. The same simulation protocol was followed with the initial structure adopted from the minimal energy configuration of the EAr·Cl^- complex corresponding to $R_\phi = 2.6$ Å.

(61) Zheng, Y.-J.; Ornstein, R. L. *J. Am. Chem. Soc.* **1997**, *119*, 648.
(62) Barshop, B. A.; Wrenn, R. F.; Froeden, C. *Anal. Biochem.* **1983**, *130*, 134.

During the simulation, the Cl^- ion stays mostly within a pocket formed by Ala86, His90, and Ile233B. The average distance between the Cl^- and the benzoyl BC4 is only 4.6 ± 0.4 Å. The absence of long-distance migration is indicative of significant barriers due to the tightness of the active site. A snapshot of the EAr·Cl^- complex is displayed in Figure 2, in which Cl^- is represented as a green ball.

From Figure 2, it is seen that the chloride ion takes the position of the water nucleophile for the hydrolysis of the aryl ester, suggesting that the Cl^- ion has to be replaced by a water molecule in order for the subsequent hydrolysis step to occur. The only possibility for this to occur is the opening of the bottom gate of the active site induced by protein fluctuation, which will permit the migration of the chloride to solvent and the incorporation of a water molecule. This speculation is reasonable, given that the halide ion is better solvated in solution than in the active site and that a possible escape route is generated by fluctuation in the side chains of His90 and/or Ala86 in an A-subunit α-helix or the side chain of Ile233 in a B-subunit α-helix. Side chain rotation can open a channel to solvent, which can be further enlarged by backbone fluctuation between the two subunits. Structural evidence seems to support the conformational flexibility of the His90 side chain. For example, the H90Q mutant shows the Gln side chain rotated out into solvent.[26] Such a scenario might explain the large ^{35}Cl kinetic isotope effect reported for dehalogenase catalyzed dechlorination of 4-CBA-CoA,[63] as the transfer of the Cl^- ion from the active site to solvent prior to hydrolysis has to overcome a significant barrier.

Indeed, our simulations of the EAr·Cl^- complex have found significant conformational changes of the His90 side chain. As shown in Figure 4, the CA−CB−CG−CD2 dihedral angle is significantly shifted from that observed in the crystal structure. In the majority of the cases, the change is about 50°, but changes as large as ∼90° (at ∼420 ps) and ∼180° (at ∼950 ps) are also seen. This is in sharp contrast to the ES complex, where the dihedral angle largely retains the crystal value of −88.5°. Furthermore, the expulsion of Cl^- ion from the benzene ring also pushes the side chain of His90 away from the active site, and the average distance between the NE2 atom of His90 and CG atom of Asp145 has changed from 4.4 to 6.0 Å. Finally, the hydrogen bond between the His90 imidazole and Ala86 backbone carbonyl seen in the ES complex is disrupted. In the presence of the Cl^- ion, the capacity of His90 as the general base catalyst would thus be greatly impaired. These conformational changes in the His90 residue are likely to result from a combination of steric and electrostatic interactions with the Cl^- ion.

Because of the stochastic boundary conditions imposed on our model, the α-helices are not entirely free to move, thus excluding the possibility of breathing motions between the A and B subunits. Indeed, the finite time constant temperature MD simulation cannot be expected to map out possible pathways for the chloride ion to leave the active site. An alternative approach to such slow dynamic events is to use the biased molecular dynamics (BMD) approach,[64] in which the dynamics is steered by a time-dependent soft ratchet defined in a given reaction coordinate. This point will be addressed soon.

(63) Lewandowicz, A.; Rudzinski, J.; Luo, L.; Dunaway-Mariano, D.; Paneth, P. *Arch. Biochem. Biophys.* **2002**, *398*, 249.
(64) Paci, E.; Karplus, M. *Proc. Natl. Acad. Sci. U.S.A.* **2000**, *97*, 6521.

In addition to the aforementioned observations, we have also detected some other conformational changes occurring in the EAr complex. The most conspicuous is that the ester carbonyl is rotated to form a hydrogen bond with the indole NH of the Trp137, as shown in Figure 3. The corresponding average O···H distance is 2.2 ± 0.3 Å. This observation is interesting, as it leaves the C_β of Asp145 open for attack by the putative water nucleophile for the subsequent hydrolysis step. We can further speculate that this hydrogen bond might play an important role in stabilizing transition states for the cleavage of the ester bond. This is consistent with experimentally observed reduction of catalytic activity in the W137F mutant.[23]

IV. Conclusions

In this work, we have investigated the dynamics and mechanism of the dechlorination reaction of 4-CBA-CoA catalyzed by 4-CBA-CoA dehalogenase, using combined QM/MM methods. The theoretical results reported in this work complement the existing experimental data. The two perspectives allow us to gain a more in-depth and systematic understanding of the catalytic power of the enzyme.

The calculated PMF strongly supports the multistep mechanism proposed by experimentalists. In particular, our results indicate the existence of a metastable EMc intermediate. Convincing evidence is presented on the redistribution of the π electrons in the benzoyl moiety during the formation of the EMc and the accompanied structural changes. These changes are consistent with the so-called "push−pull" mechanism proposed for catalysis of the S_NAr reaction. On the basis of the calculated free energy profile, we proposed a new kinetic model in which the formation of the EMc intermediate is the rate-limiting step, rather than the formation of the EAr intermediate. This kinetic model is found to be consistent with the single turnover time course of the EAr and EP complexes.

The nanosecond MD simulation of the ES complexes of the wild-type dehalogenase reveals an elaborate hydrogen bonding network in the active site. Although many key hydrogen bonds have been identified from the X-ray structure of the EP complex, some significant changes are observed for the ES complex. The most important one is the absence of the hydrogen bond between OD1 of Asp145 and NH of the Trp137 side chain, which was thought to orient the nucleophile to a favorable attacking position. Instead, the two carboxylate oxygen atoms of Asp145 form hydrogen bonds with backbone amide NH groups of Thr146 and Asp145 itself and are found to exchange positions. One of the oxygen atoms is found to be in a favorable position to attack C(4) of the substrate. In addition, hydrogen bonding is also found between the benzoyl carbonyl oxygen with backbone amide NH groups of Gly114 and Phe64. These two hydrogen bonds are strengthened during the formation of the EMc complex, indicating that they play an important role in stabilizing the transition state and the EMc intermediate relative to the gas-phase counterpart.

The simulation of the G113A mutant ES complex reveals that the presence of the methyl side chain of Ala113 pushes the substrate away from the α-helix. The structure changes result in the weakening of the electropositive forces acting on the benzoyl carbonyl, as is evidenced by the substantially elongated hydrogen bond with the Gly114 backbone amide NH. The disruption of the "oxyanion hole" seen in the simulation is

consistent with the experimentally observed larger binding constant and spectral shift of the C═O spectral line in the mutant. It ultimately leads to the destabilization of the transition states, manifested as an increased free energy barrier. The calculated change of the rate constant for the formation of EMc complex (and the EAr intermediate) is consistent with experimental observations.

The MD simulation on the WT EAr·Cl^- complex sheds light on the dynamics of the leaving group Cl^-. It is shown that during the 1 ns simulation time the ionic product is largely immobile in a receiving pocket formed by Ala86, His90, and Ile233B. However, it induces substantial structural changes in nearby residues. In particular, the side chain of His90 is found to rotate away from Asp145. The carbonyl group of the EAr complex is found to rotate to form a hydrogen bond with the indole NH of Trp137, which might have important implications in hydrolysis. We propose that the Cl^- ion is released into the solvent by conformationally induced opening of the bottom of the active site. It is conceivable that this is accompanied by the diffusion of a water molecule into the active site, which will serve as the nucleophile in the ensuing hydrolysis step.

Acknowledgment. This work was funded by the National Science Foundation (H.G. and Q.C.) and National Institutes of Health (D.D.M. and J.G.). Q.C. would also like to thank the Alfred P. Sloan foundation for a Research Fellowship. We thank Mr. Xuefeng Lu for technical assistance.

JA0460211